Solution and Solid-State Conformational and Structural Analysis of the *N*-Methyl Derivatives of (±)-*threo*-Methylphenidate, (±)-*erythro*-Methylphenidate, and (±)-*threo*-*p*-Methyl-methylphenidate Hydrochloride Salts

Robert Glaser,*[,†,‡] Itay Adin,[†] and Dror Shiftan[†]

Department of Chemistry, Ben-Gurion University of the Negev, Beer-Sheva 84105, Israel and The Institute for Advanced Studies at the Hebrew University of Jerusalem, Jerusalem 91904, Israel

Qing Shi and Howard M. Deutsch

School of Chemistry and Biochemistry, Georgia Institute of Technology, Atlanta Georgia 30332-0400

Clifford George

Laboratory for the Structure of Matter, Naval Research Laboratory, Washington, D.C. 20375-0001

Kuo-Ming Wu and Mark Froimowitz

Pharm-Eco Laboratories, 128 Spring Street, Lexington, Massachusetts 02173-7800

Received June 12, 1997 (Revised Manuscript Received December 19, 1997)

The conformational preferences of *N*-methyl derivatives of the dopamine reuptake blocker *threo*-methylphenidate [Ritalin] and the *p*-methyl analogue were determined in the solid state and in solution and that of the *erythro* isomer in solution. The solid-state structures of (±)-*threo*-*N*-methyl-α-phenyl-2-piperidineacetic acid methyl ester hydrochloride [(±)-*threo*-*N*-methyl-methylphenidate hydrochloride] (**2**) and (±)-*threo*-*N*,*p*-dimethyl-α-phenyl-2-piperidineacetic acid methyl ester hydrochloride (**5**) were determined by single crystal X-ray diffraction analysis. (±)-**2** underwent spontaneous resolution to give crystalline chiral plates containing two independent molecules in the asymmetric ring, and at each site there is a disorder involving the *N*-methylpiperidinyl ring methylene and methyl carbon atoms with a 0.710(7):0.290(7) ratio of occupancy factors. The two (2*RS*,3*RS*,4*SR*) major disordered molecules have similar structures consisting of a *chair* conformation for the piperidine ring with *axial N*-methyl and CH(Ph)COOMe groups. The two (2*RS*,3*RS*,4*RS*) minor molecules in the disorder also have similar structures and differ from the major ones by epimerization at nitrogen and inversion of the piperidine ring to afford an *axial N*-methyl group, and an *equatorial* CH(Ph)COOMe group. (±)-**5** gave crystalline plates also containing *diaxially* disposed piperidinyl-ring substituents. Dissolution in D_2O of either **2** or its *erythro*-epimer (**3**) each gives a 5:4 ratio of two species in which the major species exhibits an *axial* N-methyl group and an *equatorial* CH(Ph)COOMe group while the minor species has a *diequatorial* arrangement for both substituents. Both of the *axial N*-methyl *threo* or *erythro* major species in D_2O are overwhelmingly conformationally biased in favor of an *antiperiplanar* H(2)···H(3) disposition and one piperidine ring invertomer. Dissolution of the *threo* or *erythro* epimers in CD_2Cl_2 gives the same *axial N*-methyl/*equatorial* CH(Ph)COOMe and *diequatorially* disposed species but now in a reversed ratio [respectively 3:20 for *threo* and 4:5 for *erythro*].

Introduction

Methylphenidate hydrochloride [Ritalin, (2*RS*,3*RS*)-α-phenyl-2-piperidineacetic acid methyl ester hydrochloride,[1] **1**], which is in common use as a treatment for attention deficit hyperactivity disorder,[2] is a dopamine reuptake blocker with stimulant properties that was first synthesized[3] more than 50 years ago. The stimulant activity resides in the *threo* isomer,[4] and the (2*R*,3*R*)-absolute configuration[2,5] has been ascertained for the more active enantiomer.

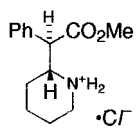

1

Recently, there has been a revival of interest in methylphenidate and its analogs due to its common mechanism of action with cocaine, a major drug of abuse in the United States. A conformational analysis of the *threo* and *erythro* isomers was performed with MM2-87

† Ben Gurion University.
‡ Institute for Advanced Studies.

(1) *The Merck Index,* 11th ed.; Budavari, S., Ed.; Merck: Rahway, 1989; p 960 and references therein.
(2) Froimowitz, M.; Patrick, K. S.; Cody, V. *Pharm. Res.* **1995**, *12,* 1430, and references therein.
(3) Pannizzon, L. *Helv. Chim. Acta* **1944**, *27,* 1748.
(4) Szporny, L.; Görög, P. *Biochem. Pharmacol.* **1961**, *8,* 263.
(5) Shafi'ee, A.; Hite, G. *J. Med. Chem.* **1969**, *12,* 266.

S0022-3263(97)01063-3 CCC: $15.00
Published on Web 02/26/1998

(2*R*,3*R*,*M*)-**1** (2*R*,3*R*,4*S*,*M*)-**2**

Figure 1. Iconic projections of **1** and of the corresponding molecular model of the *equatorial N*-methyl diastereomer of **2** based on X-ray crystallographically determined structure[2] of (2*S*,3*S*,*P*)-**1**.

calculations, and the first crystal structure of the *threo* isomer was reported, confirming the absolute configuration of the active enantiomer.[2] The preferred conformer for *threo*-methylphenidate appeared to be one with a hydrogen bond between the carbonyl oxygen and an *equatorial* ammonium proton, see (2*R*,3*R*,*M*)-**1** in Figure 1. In addition, a pharmacophore model of dopamine reuptake blockers was recently proposed[6] and the active enantiomer of *threo*-methylphenidate was incorporated into the model. Independently of this, a series of methylphenidate analogs with different substitutions on the phenyl ring was reported.[7] As with other dopamine reuptake blockers, halogen substitutions in the *meta* and *para* positions greatly increased activity.

The incorporation of **1** into the pharmacophore model suggested that the *N*-methyl derivative of methylphenidate should have decreased activity since an *equatorial N*-methyl group would occupy the position required for an ammonium hydrogen as defined by the pharmacophore model, see (2*R*,3*R*,4*S*,*M*)-**2** in Figure 1.[6] This was found to be the case in that *N*-methyl derivatives of analogues with varying phenyl substitutions were 4−30 fold less active than the corresponding secondary amines.[8] However, there is a complication to all of this in that *N*-methyl derivatives of *threo*-methylphenidate were found to have a complex conformational equilibrium highly dependent on the molecular environment.[8] Here we report the results of conformational studies of (±)-*N*-methyl-α-phenyl-2-piperidineacetic acid methyl ester hydrochloride [*N*-methyl-methylphenidate hydrochloride, **2**] by NMR spectroscopy and X-ray crystallography. In addition, the *erythro* isomer **3** was also found to have multiple conformations, and we report a conformational analysis of this compound using NMR spectroscopy.

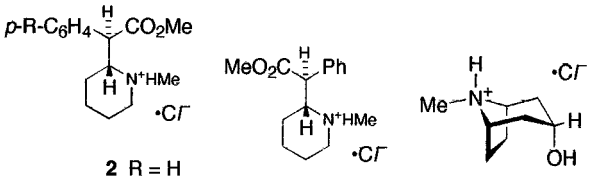

2 R = H
5 R = Me
3
4

The NMR observation of *N*-methyl diastereomers is linked to the lifetimes of the two species on the NMR time-scale of measurement. One of the earliest reports concerns the 40 MHz ^{1}H NMR investigation at the slow exchange limit (SEL) for diastereomerization of tropine hydrochloride (**4**) in acidic water.[9] An aqueous solution (pD 1) of this compound afforded a *ca.* 16:1 preference of *equatorial N*-methyl (8*s*)-isomer over the *axial* (8*r*)-epimer.[9] Increasing the pH to neutrality afforded weighted time-averaged resonances for the two diastereomers at the fast exchange limit (FEL) for interconversion.[9] The acidity of the aqueous medium is not a prerequisite for the observation of *N*-methyl diastereomeric species, especially when the measurements are performed at higher field strengths. Each of the *threo* [(2*RS*,3*RS*)] and *erythro* [(2*SR*,3*RS*)] *N*-methyl-methylphenidate hydrochloride diastereomers (**2** and **3**, respectively) and also the (±)-*threo*-*N*,*p*-dimethyl-α-phenyl-2-piperidineacetic acid methyl ester hydrochloride (**5**) derivative afforded ^{1}H NMR [300 and 500 MHz] spectra showing two *N*-methyl diastereomers in neutral D_2O. These observations were an important impetus for undertaking the stereochemical studies reported herein.

Another method of increasing the NMR time-scale lifetimes of *N*-methyl diastereomeric salt species in ambient temperature equilibrium involves the use of a chlorinated organic solvent, *e.g.* CD_2Cl_2. This solvent has an advantage over D_2O in that vicinal coupling constants involving the *N*-proton are readily observed, and, as a result, important stereochemical information is not lost in the ^{1}H NMR spectrum due to the exchange of this proton by deuterium.[10,11] Vicinal coupling constants involving ^3J(N*H*C*H*) enabled the differentiation of (+)-*synclinal* versus (−)-*synclinal* conformational models for the *NC*H_2*C*H_2*C* fragment in the major and minor species of (+)-glaucine hydrofluoroacetate alkaloid salt.[11] In the NMR investigations of **2** and **3** reported below, two solvents (D_2O and CD_2Cl_2) were used to study the solution-state equilibria of *N*-methyl analogues of *threo*- and *erythro*-methylphenidate.

Results

The solid-state structures of **2** and **5** were determined by single crystal X-ray diffraction analysis.[12] The bend of a particular piperidine ring invertomer can be denoted by a (*P*) or (*M*)-descriptor for the sign of one of the *synclinal* (*gauche*, *ca.* 60°) torsion angles in the ring which, while arbitrary, is consistently applied throughout this work, *e.g.* torsion angle C(8)−C(3)−N−C(5) [see numbering scheme in structures **6**, **7**]. For **2**, there are two independent structures (composite **6** and **6′**) in the asymmetric unit and at each site there is a disorder [0.710(7):0.290(7) ratio of occupancy factors] involving *N*-methylpiperidinyl-ring C(5−8) methylene and C(9) methyl carbon atoms, see composite **6**. The major

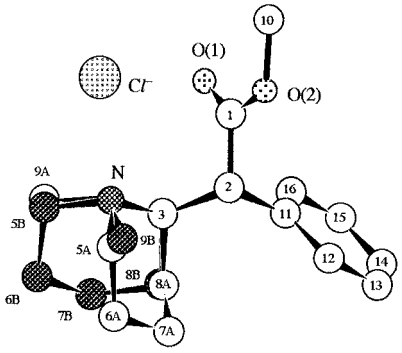

6

(6) Froimowitz, M. *J. Comput. Chem.* **1993**, *14*, 934.
(7) Deutsch, H. M.; Shi, Q.; Gruszecka-Kowalik, E.; Schweri, M. M. *J. Med. Chem.* **1996**, *39*, 1201.
(8) Froimowitz, M.; Deutsch, H. M.; Shi, Q.; Wu, K.-W.; Glaser, R.; Adin, I.; George, C.; Schweri, M. M. *Bioorg. Med. Chem. Lett.* **1997**, *7*, 1213.

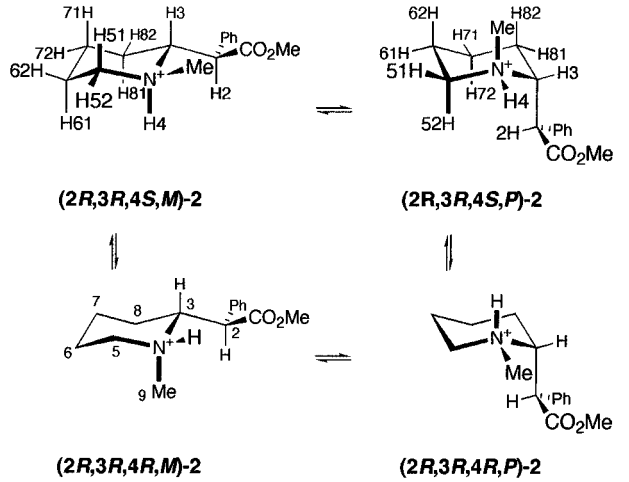

Figure 2. Interconversion of diastereomeric ammonium cations **2** by the prototropic-shift/nitrogen inversion mechanism (vertical pathways) and by ring-inversion (horizontal pathways).

components (**2-A**, **2′-A**) at the two sites of disorder have (2*RS*,3*RS*,4*SR*,*PM*)-descriptors. These molecules have very similar structures as shown by the small 0.025 Å root-mean-squared (RMS) difference in their superimposition.[13] The structure consists of a *chair* conformation for the piperidine ring with an *axial* oriented *N*-methyl group, an *axial* oriented CH(Ph)COOMe moiety, an *antiperiplanar* (*ca.* 180°) arrangement of the two vicinal methine-protons about the C(2)−C(3) bond, a 26° shallow *synclinal* value of the H(2)−C(2)−C(1)−O(2) torsion angle [see partial numbering in **6**], and the phenyl ring eclipsing the C(2)−H(2) bond [see (2*R*,3*R*,4*S*,*P*)-**2** in Figure 2 and the white colored A-denoted piperidine ring atoms in **6**]. The minor components (**2-B**, **2′-B**) at the two sites of disorder have (2*RS*,3*RS*,4*RS*,*MP*)-descriptors. These molecules also have similar structures (0.061 Å RMS difference). The two minor components differ from those of the two major ones by epimerization at nitrogen and inversion of the piperidine ring to afford an *axially* oriented *N*-methyl group, and an *equatorially* oriented CH(Ph)COOMe moiety [see (2*R*,3*R*,4*R*,*M*)-**2** in Figure 2 and the black colored B-denoted piperidine ring atoms in **6**].

The structure of **5** is almost identical to the two major component (2*RS*,3*RS*,4*SR*,*PM*)-diastereomers of **2**, which also have *diaxially* disposed piperidinyl-ring substituents, and is depicted in ball and stick structure **7**. This is seen by the 0.130 Å RMS diffrerence value for the superimposition of **5** upon each of the *diaxial* molecules **2-A** and **2′-A** in the disorder. If the five aromatic carbons of **5** are removed from the superimposition, then the RMS difference markedly improves to a value of 0.040 Å [for **2-A**] and 0.039 Å [for **2′-A**]. Therefore, the main difference in the conformation of **5** versus those in **2-A**,**2′-A** is in the pitch of the aromatic ring [the C(3)−C(2)−C(11)−C(12) torsion angle is −121.6(4)° for **5**, −110.7(5)° for **2-A**, and −111.5(5)° for **2′-A**]. Structures **2-A**, **2′-A** and **5** all show an *antiperiplanar*-type 166(2)° H(2)−C(2)−C(3)−H(3) value conformational arrangement in which the smallest substituent on C(2), *i.e.* H(2), is pointing into the cleft between two *axial* piperidine ring protons [see (2*R*,3*R*,4*S*,*P*)-**2** in Figure 2]. A similar conformation about the C(2)−C(3) bond is found by X-ray crystallography not only for the two independent **2-A**, **2′-A** molecules but also for the *N*-desmethyl parent[2] (**1**) as shown by relatively low RMS differences of 0.137, 0.138, 0.079 Å for the superimposition of N,C(2,3,8,10−16), and the two O-atoms of **5** upon those corresponding atoms in **2-A**, **2′-A**, and **1**. The CH(Ph)COOMe moiety is *equatorially* disposed in **1** (see Figure 1).[2]

In molecules **2-B** and **2′-B** of the disorder, the *antiperiplanar* disposition of the two vicinal methine-protons about the C(2)−C(3) bond places the C(2)−H(2) bond parallel to the N−C(9) bond [see (2*R*,3*R*,4*R*,*M*)-**2** in Figure 2]. In this spatial arrangement, (+)-*gauche*/(−)-*gauche* interactions (g^+/g^-, also termed *syn*-pentane interactions), are avoided between the *axial* *N*-methyl group and either of the phenyl or methoxycarbonyl moieties.[14] This interaction is well-known in the form of *cis*-1,3-*diaxial* interactions in cyclohexane derivatives.[14]

NMR Spectroscopy. The ^{1}H [500 MHz] and ^{13}C [125 MHz] NMR (CD_2Cl_2 or D_2O) spectral parameters for a mixture of *N*-methyl diastereomers at the SEL for interconversion are listed in Tables 1 and 2 for **2**, **3**, and **5**. The numbering scheme of protons is given in Figure 2. Descriptors differentiating protons in an internally diastereotopic pair are given in the same manner as that commonly used in X-ray crystallography, *e.g.* nuclei H(51) and H(52) are both ligated to C(5).

Two species of each compound were clearly seen in both ^{1}H and ^{13}C NMR spectra of the salts dissolved in either CD_2Cl_2 or D_2O. In CD_2Cl_2 the *N*-methyl diastereomeric ratio was 20:3 for the *threo* isomer (**2**), and 5:4 for the *erythro* epimer (**3**), while in D_2O the same *N*-configurational species were in a ratio of 4:5 for each one of the salts **2**, **3**, **5**. All the **2**, **3**, and **5** salts studied afforded sharp ^{13}C signals when measured in neutral D_2O solutions. Fine structure was readily observed for ^{1}H resonances in both the *N*-methyl diastereomers of **3** and **5**. However, the particular sample of **2** investigated afforded

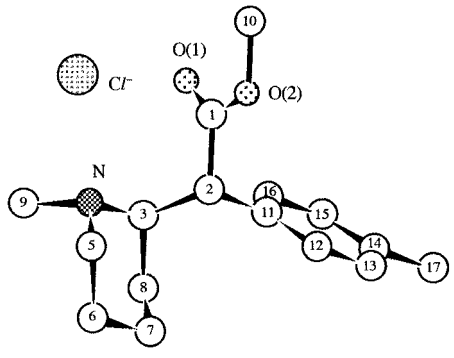

7

(9) Closs, G. L. *J. Am. Chem. Soc.* **1959**, *81*, 5456.
(10) Glaser, R.; Blumenfeld, J.; Geresh, S. *Magn. Reson. Chem.* **1993**, *31*, 845.
(11) Glaser, R.; Bernstein, M. A. *J. Chem. Soc., Perkin Trans. 2* **1991**, 2047.
(12) The authors have deposited atomic coordinates for these structures with the Cambridge Crystallographic Data Centre. The coordinates can be obtained, on request, from the Director, Cambridge Crystallographic Data Centre, 12 Union Road, Cambridge, CB2 1EZ, U.K.
(13) Sundin, A. *MacMimic 3.0*, In-Star Software: Lund, Sweden, 1996.
(14) Hoffmann, R. W. *Angew. Chem., Int. Ed. Engl.* **1992**, *31*, 1124, and references therein.

Table 1. Aliphatic ^{1}H NMR Partial Spectral Parameters for *N*-Methyl Diastereomers of Salts 2, 3, and 5[a]

	equat. N-Me equat CH(Ph)COOMe (2*RS*,3*RS*,4*SR*,*MP*)-**2**		*axial N-Me equat CH(Ph)COOMe* (2*RS*,3*RS*,4*RS*,*MP*)-**2**		*equat. N-Me equat CH(Ph)COOMe* (2*SR*,3*RS*,4*SR*,*MP*)-**3**		*axial N-Me equat CH(Ph)COOMe* (2*SR*,3*RS*,4*RS*,*MP*)-**3**	
	CD_2Cl_2 major	D_2O minor	CD_2Cl_2 minor	D_2O major	CD_2Cl_2 major	D_2O minor	CD_2Cl_2 minor	D_2O major
				δ H[b]				
H(2)	4.53	4.29 [4.31]	3.97	3.91 [3.93]	4.54	4.63	4.49	3.96
H(3)	3.78	3.86 [3.89]	–	3.95 [3.97]	3.36	3.54	3.72	4.15
H(4), NH	12.69	*c* [*c*]	12.59	*c* [*c*]	12.47	*c*	12.56	*c*
H(51)	2.85	3.02 [3.07]	–	3.28 [3.38[d]]	2.75	2.98	–	3.25
H(52)	3.42	3.34 [3.42]	–	3.28 [3.32[d]]	3.40	3.42	3.17	3.11
H(61)	2.11	– [1.80[d]]	–	1.69[d] [1.76[d]]	2.24[d]	–	1.89[d]	1.82[d]
H(62)	1.76	– [1.50[d]]	–	1.57[d] [1.63[d]]	1.79[d]	–	1.78[d]	1.70[d]
H(71)	1.35	1.34[d] [1.42[d]]	–	– [1.61[d]]	1.45[d]	1.32[d]	1.87[d]	1.56[d]
H(72)	1.76	– [1.64[d]]	–	– [1.64[d]]	1.93[d]	1.73[d]	2.14[d]	1.82[d]
H(81)	1.67	1.71[d] [1.76[d]]	–	– [1.25[d]]	2.16[d]	1.91[d]	1.46[d]	–
H(82)	1.17	1.18[d] [1.26[d]]	–	– [1.21[d]]	2.05[d]	1.77[d]	2.14[d]	–
NCH_3	2.71	2.85 [2.90]	2.40	2.75 [2.79]	2.41	2.91	2.55	2.65
OCH_3	3.69	3.55 [3.62]	3.77	3.57 [3.60]	3.72	3.70	3.68	3.59
CCH_3	*c*	*c* [2.23]	*c*	*c* [2.22]	*c*	*c*	*c*	*c*
				J_{HH}[e]				
2–3	8.6(2)	7.7(1) [7.6(2)]	9.9(1)	11.0(1) [11.2(1)]	8.2(3)	5.9(3)	6.0(1)	11.6(1)
3–4	8.3(2)	*c c*	–	*c c*	8.7(4)	*c*	–	*c*
3–81	12.1(2)	8.2(3) [8.8(1)]	–	11.4(1) [11.3(2)]	11.5(3)	9.0(5)	–	11.3(1)
3–82	3.2(2)	3.1(3) [3.1(3)]	–	2.5(1) [2.4(3)]	3.0(3)	3.4(5)	–	2.3(1)
4-CH_3	4.9(1)	*c c*	4.8(1)	*c c*	4.7(1)	*c*	5.0(1)	*c*
4–51	9.4(2)	*c c*	–	*c c*	9.2(2)	*c*	3.6(5)	*c*
4–52	1.6(1)	*c c*	–	*c c*	–	*c*	–	*c*
51–52	−12.4(1)	−12.9(2) [−13.0(1)]	–	– –	−12.6(2)	−12.8(4)	−13.4(5)	−13.2(2)
51–61	12.7(2)	9.6(1) [9.6(1)]	–	– –	12.6(2)	10.3(4)	10.4(5)	13.2(2)
51–62	3.1(3)	3.4(1) [3.4(1)]	–	– –	3.1(2)	3.0(3)	3.4(5)	3.0(3)
52–61	4.1(2)	– –	–	– –	4.0(1)	4.1(2)	–	2.5(3)
52–62	2.4(1)	– –	–	– –	–	4.1(2)	–	2.5(3)
52–72	2.4(1)	– –	–	– –	–	–	–	–
61–62	–	– –	–	– –	−13.7(6)	–	–	–
61–71	11.5(3)	– –	–	– –	13.7(6)	–	–	–
61–72	–	– –	–	– –	4.0(1)	–	–	–
62–82	3.0(4)	– –	–	– –	–	–	–	–
71–72	−13.0(3)	– –	–	– –	–	–	–	–
71–81	12.9(3)	– –	–	– –	–	–	–	–
71–82	3.0(4)	– –	–	– –	–	–	–	–
72–81	3.4(1)	– –	–	– –	–	–	–	–
72–82	3.0(4)	– –	–	– –	–	–	–	–
81–82	−14.6(1)	– –	–	– –	–	–	–	–

[a] Ratios in CD_2Cl_2 of *equatorial:axial N*-methyl diastereomeric (2*RS*,3*RS*,4*SR*,*MP*)-**2**:(2*RS*,3*RS*,4*RS*,*MP*)-**2** and (2*SR*,3*RS*,4*SR*,*MP*)-**3**:(2*SR*,3*RS*,4*RS*,*MP*)-**3** species are 20:3 and 5:4, respectively, and 4:5 for both *threo* and *erythro* compounds in D_2O, data for **5** given in square brackets. [b] Ppm downfield from tetramethylsilane or 4,4-dimethyl-4-silapentanesulfonate sodium salt, 500 MHz. [c] Not applicable. [d] Internally diastereotopic pairs [H(X1,X2)] were located in the HMQC 2D-NMR correlation spectrum, and their relative assignments may be reversed. [e] Hz, estimated standard deviation of last digit given in parentheses.

Table 2. Aliphatic ^{13}C NMR Spectral Parameters for *N*-Methyl Diastereomers of Salts 2, 3, and 5[a,b]

	equat N-Me equat CH(Ph)COOMe (2*RS*,3*RS*,4*SR*,*MP*)-**2**		*axial N-Me equat CH(Ph)COOMe* (2*RS*,3*RS*,4*RS*,*MP*)-**2**		*equat N-Me equat CH(Ph)COOMe* (2*SR*,3*RS*,4*SR*,*MP*)-**3**		*axial N-Me equat CH(Ph)COOMe* (2*SR*,3*RS*,4*RS*,*MP*)-**3**	
	CD_2Cl_2 major	D_2O minor	CD_2Cl_2 minor	D_2O major	CD_2Cl_2 major	D_2O minor	CD_2Cl_2 minor	D_2O major
C(1)	173.94	173.45 [173.69]	173.94	173.16 [173.40]		172.27		172.32
C(2)	52.75	50.80 [50.44]	51.42	51.47 [51.14]	53.72	49.56	51.47	52.57
C(3)	66.16	64.80 [64.87]	62.85	63.16 [63.22]	68.55	66.12	65.35	63.22
C(5)	57.57	54.79 [54.83]	53.87	55.33 [55.37]	59.25	55.64	54.57	55.41
C(6)	23.13	21.08 [21.23]	19.95	17.19 [17.33]	23.41[c]	21.58[c]	19.72	17.00
C(7)	22.86	19.68 [19.80]	20.53	21.13 [21.17]	23.09[c]	20.25[c]	22.02[c]	21.35[c]
C(8)	27.95	24.44 [24.51]	23.62	21.22 [21.35]	27.50	23.25	22.14[c]	22.14[c]
NCH_3	41.63	41.00 [41.04]	36.65	32.82 [32.89]	44.28	40.87	36.12	32.02
OCH_3	53.44	53.37	53.44	53.47 [53.41]	53.23	52.92	53.00	53.06
CCH_3	na[d]	na[d]	na[d]	na[d] [20.20]	na[d]	na[d]	na[d]	na[d]

[a] Ratios in CD_2Cl_2 of *equatorial:axial N*-Methyl diastereomeric (2*RS*,3*RS*,4*SR*,*MP*)-**2**:(2*RS*,3*RS*,4*RS*,*MP*)-**2** and (2*SR*,3*RS*,4*SR*,*MP*)-**3**:(2*SR*,3*RS*,4*RS*,*MP*)-**3** species are 20:3 and 5:4, respectively, and 4:5 for both *threo* and *erythro* compounds in D_2O; data for **5** given in square brackets. [b] Ppm downfield from tetramethylsilane or 4,4-dimethyl-4-silapentanesulfonate sodium salt, 125 MHz. [c] Assignments may be reversed. [d] Not applicable.

exchange broadened ^{1}H resonances for *each* of the two species which then sharpened-up upon addition of one drop of trifluoroacetic acid (TFA) to the *ca.* 0.5 mL of D_2O solution. Similar, but more severe, exchange broadened behavior, and subsequent sharpening upon TFA addition was noted in the ^{13}C NMR (D_2O) spectrum of (−)-scopolamine hydrobromide (**8**) due to its lowered 7.55[16] pK_a value.[15] A more typical pK_a value for protonated amines is *ca.* 9.3.[16]

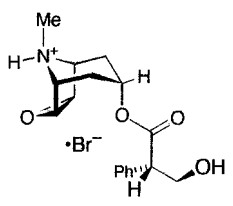

8

Table 3. Molecular Mechanics Steric Energies, Characteristic Torsion Angles, and Boltzmann Distribution of MM3 Calculated C(2)−C(3) Bond Rotameric Models for *N*-Methyl Diastereomers of Salts 2 and 3

N-Me and CH(Ph)COOMe dispositions	angle C(1)−C(2)−C(3)−C(8)[a]	angle O(2)−C(1)−C(2)−C(3)[a]	angle H(2)−C(2)−C(11)−C(12)[a]	angle H(2)−C(2)−C(3)−H(3)[a]	estimated ^3J(H2H3)[b]	steric energy[c]	Boltzmann distribution[d]
equat equat	71	175	21	65	2.2	22.5	48.2
(2*R*,3*R*,4*S*,*M*)-**2**	−68	156	52	−70	1.4	24.3	9.6
	164	−156	3	164	11.1	22.6	42.2
axial equat	72	173	6	67	2.0	26.5	1.3
(2*R*,3*R*,4*R*,*M*)-**2**	−50	175	33	−51	4.0	25.2	0.5
	177	166	7	−177	12.0	21.6	98.2
axial axial	69	173	19	64		28.8	
(2*R*,3*R*,4*S*,*P*)-**2**	−58	160	28	−55		32.5	
	−179	167	6	180		22.6	
	[164(1)/165(1)][e]	[145/146][e]	[9/9][e]	[165/164][e]			
	{168}[e]	{146}[e]	{−2}[e]	{168}[e]			
equat axial	72	171	20	67		27.6	
(2*R*,3*R*,4*R*,*P*)-**2**	−62	142	44	−59		33.0	
	168	149	−1	170		24.1	
equat equat	55	−150	8	177	11.9	23.6	12.9
(2*S*,3*R*,4*S*,*M*)-**3**	−70	−170	−31	52	4.3	21.5	84.0
	160	169	−20	−68	1.5	25.2	3.1
axial equat	64	−162	1	−175	12.0	22.5	95.1
(2*S*,3*R*,4*R*,*M*)-**3**	−51	−159	−26	71	1.6	26.4	3.0
	173	−163	−38	−57	2.9	26.9	1.9
axial axial	65	−162	−2	−174		23.3	
(2*S*,3*R*,4*S*,*P*)-**3**	−66	−147	−25	58		31.8	
	170	−164	−25	−59		28.2	
axial equat	59	−156	1	−179		24.3	
(2*S*,3*R*,4*R*,*P*)-**3**	−70	−149	−27	54		30.1	
	156	177	−19	−69		30.8	

[a] Degrees. [b] Hertz, calculated according to ref 30. [c] kcal/mol, dielectric constant = 80. [d] Percent calculated at 298 K. [e] Corresponding angles in the X-ray crystallographically determined structures of molecule 1 (**2**) and molecule 2 (**2′**) [in square brackets] and of **5** {in braces}.

In CD_2Cl_2 solutions of **2**, all the ^{1}H signals of the major species were resolved in a 500 MHz spectrum with the exception of those from the piperidinyl H(62) and H(72) nuclei. Broadened *N*-H singlets were found in a ratio of 20:3 for the major and minor species of **2**, and 5:4 for the major and minor species of **3**.

Discussion

Stereochemistry. Epimers **2** and **3** contain three chirotopic stereogenic[17] atoms: the stereostable C(2) and C(3) methine carbons and the stereolabile nitrogen. For each of the separated *threo*- or *erythro*-diastereoisomers there are two stereogenic elements in addition to C(2) and C(3): the bend of the piperidine ring and the tetrahedral-type nitrogen atom. Arbitrarily keeping the conformational arrangement about the C(2)−C(3) bond invariant, these two elements give rise to four *threo*-diastereomers [(2*R*,3*R*,4*S*,*M*)-**2**, (2*R*,3*R*,4*S*,*P*)-**2**, (2*R*,3*R*,4*R*,*P*)-**2**, and (2*R*,3*R*,4*R*,*M*)-**2**] illustrated in Figure 2 and their corresponding enantiomers. One can envision two kinetic processes for diastereomer interconversion: (1) a prototropic-shift/nitrogen inversion involving vertical pathways, and (2) ring-inversion of the piperidinyl-ring *chair* conformation involving horizontal pathways. The vertical pathways keep the piperidine ring conformation invariant, but change the configuration at nitrogen, while the horizontal pathways invert the ring conformation and interchange the *equatorial*/*axial* dispositions of ring-substituents while keeping the nitrogen configuration unchanged.

MM3(92)[18] geometry optimization calculations were performed with a dielectric constant (DE) of 80. A high dielectric constant was utilized to reduce possible over-emphasis in intramolecular hydrogen-bonding interactions in the absence of explicit solvent molecules which would be able to form competitive hydrogen bonds. Three *staggered* C(2)−C(3) bond rotameric models were calculated for each of the four cationic *threo*-diastereomers illustrated in Figure 2 as well as another set of three for each of the corresponding four *erythro* analogues. The results of these modeling studies are presented in Table 3. Iconic projections of the important *threo*-diastereomer molecular models (**9**, **11**, **13**) and *erythro*-epimer models (**10**, **12**) are depicted in Figure 3. MM3(92) computational results have previously been presented for the *threo* isomer[8] but the present results were recomputed using a different software package.

The molecular modeling results for **2** in Table 3 show that the *axial N*-methyl/*equatorial* CH(Ph)COOMe species **9** has the lowest conformational energy. However, *equatorial*/*equatorial*, *axial*/*equatorial*, and *axial*/*axial* species are within 1 kcal/mol. The experimental observation of *axial*/*equatorial* as the major species in D_2O, the *diequatorial* as the major species in CD_2Cl_2, and the *diaxial* species in the crystal state is consistent with their low computed energies. For the *erythro* isomer **3**, an *equatorial*/*equatorial* species has the lowest energy and an *axial N*-methyl/*equatorial* CH(Ph)COOMe species is 1.0 kcal/mol higher in energy. These two species are also the ones observed by NMR spectroscopy.

As expected for species in **2** and **3** with an *axial* CH(Ph)COOMe group, only *antiperiplanar* H(2)···H(3) rotamers afforded low energy structures since this minimizes *cis*-1,3-*diaxial* steric interactions by placing H(2), the

(15) Glaser, R.; Peng, Q.-J.; Perlin, A. S. *J. Org. Chem.* **1988**, *53*, 2172.

(16) Newton, D. W.; Kulza, R. B. In *Principles of Medicinal Chemistry*, 2nd ed.; Foye, W. O., Ed.; Lea and Febinger: Philadelphia, 1981; p 901.

(17) Mislow, K.; Siegel, J. *J. Am. Chem. Soc.* **1984**, *106*, 3319.

(18) *MM3(92) for the Macintosh*/*PowerMac 2.0*, In-Star Software: Lund, Sweden, 1996.

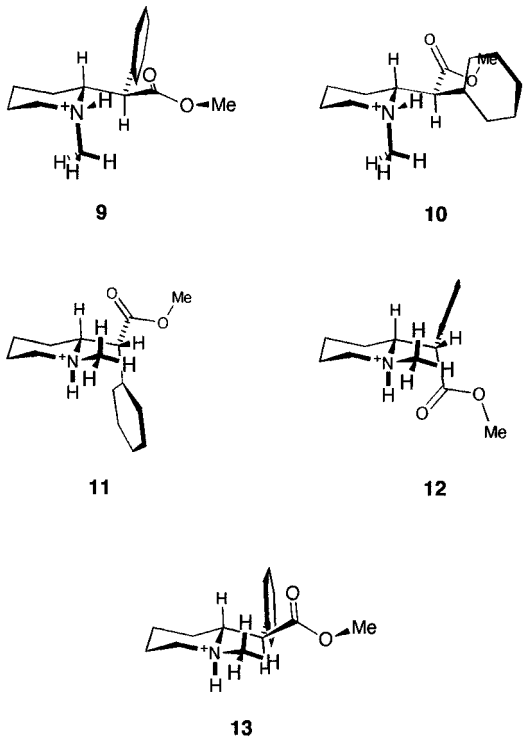

Figure 3. Iconic projections of MM3-minimized models of species observed by NMR spectroscopy. For **2**, these are the *N*-methyl *axial* (**9**) and *equatorial* (**11**, **13**) species and the *N*-methyl *axial* (**10**) and *equatorial* (**12**) species for **3**.

smallest group attached to C(2), toward the ring interior. High 298 K Boltzmann distributions[19] for *antiperiplanar* H(2)···H(3) rotamers are estimated for *axial N*-methyl/*equatorial* CH(Ph)COOMe species [*ca.* 98% for model **9** of (2*R*,3*R*,4*R*,*M*)-**2** and *ca.* 95% for model **10** of (2*S*,3*R*,4*R*,*M*)-**3**]. While possible overestimation of internal hydrogen-bonding in a particular MM3 model conformation might still arise even when DE = 80 [*e.g.* model **9**], reduction of piperidine *cis*-1,3-*diaxial* interactions is a very important driving force for C(2)−C(3) bond rotational equilibria as shown by the high estimated population for model **10**, where this is not possible.

Also as expected, high 298 K Boltzmann distribution populations were estimated for (+)-*synclinal* H(2)···H(3) models of *equatorial N*-methyl/*equatorial* CH(Ph)COOMe species having g^+/g^- interactions[14] minimized by coplanar juxtapositions of the C(2)−H(2) and N−CH_3 bonds [*ca.* 48% for model **11** of (2*R*,3*R*,4*S*,*M*)-**2** and *ca.* 84% for model **12** of (2*S*,3*R*,4*S*,*M*)-**3**]. While models **9** and **11** represent the predominant C(2)−C(3) bond rotamer for the respective (2*R*,3*R*,4*R*,*M*)-**2** and (2*R*,3*R*,4*S*,*M*)-**2** diastereomers, a second rotamer for the latter also appears to be significantly populated [42% *antiperiplanar* H(2)···H(3) (model **13**)] giving an estimated combined population of *ca.* 90% for non-internally hydrogen-bonded models **11** and **13** of (2*R*,3*R*,4*S*,*M*)-**2**.

Superimposition of the non-hydrogen atoms in the *axial N*-methyl/*axial* CH(Ph)COOMe (2*R*,3*R*,4*S*,*P*)-**2** model upon corresponding atoms in the X-ray crystallographically determined structures of **2-A**, **2′-A**, and **5** gave respective RMS differences of 0.297, 0.295, and 0.262 Å. The geometry of the calculated *diaxial* model appears to be similar to those of the three X-ray crystallographically determined structures though with the carbonyl oxygen atom more inclined toward the nitrogen in the model, despite the high dielectric constant in the calculations. Distance O(1)···N is 2.26 Å in the model versus 2.848, 2.879, and 3.037 Å in the respective **2-A**, **2′-A**, and **5** X-ray structures. However, if the **2-A** X-ray determined structure (including the Cl anion) is used as the starting structure for geometry optimization with fixed N^+−H···Cl^- atoms, then the O(1)···N distance in the model opens up to 2.63 Å. The presence of the hydrogen-bonded chloride anion in the new (2*R*,3*R*,4*S*,*P*)-**2** model improved the superimposition of its non-hydrogen/non-chlorine atoms upon those in **2-A**, **2′-A**, and **5** [respective RMS difference decreases to 0.188, 0.191, and 0.152 Å].

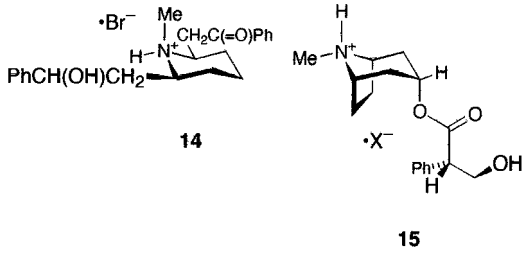

Solid-state cpmas ^{13}C NMR spectroscopy combined with crystallographic structure determination may be used to characterize the stereochemistry of solution-state molecules at the SEL to interconversion and also that of the predominant species at the FEL for exchange. For example, crystallography has shown that the *N*-methyl groups in crystalline (−)-α-lobeline hydrobromide (**14**)[20] and (−)-scopolamine hydrobromide sesquihydrate[21] (**8**·1.5H_2O) are *axial*, while they are *equatorial* in crystalline (−)-hyoscyamine hydrobromide[22] (**15**, X^- = Br^-) [atropine is racemic hyoscyamine] and (+)-phendimetrazine bitartarate[23] (**16**, X^- = $C_4H_5O_6^-$). Solid-state cpmas ^{13}C NMR spectroscopy has shown that the resonances of *axial N*-methyl carbon nuclei are characteristically shifted upfield [*e.g.* δ 30.90[20] and 31.85[15,24] for crystalline **14** and **8**·1.5H_2O, respectively] relative to corresponding signals for *equatorial N*-methyl carbons [*e.g.* δ 40.76[24] and 42.74[25] in crystalline **15** (X^- = Br^-) and **16** (X^- = $C_4H_5O_6^-$), respectively]. These relative values can be used to assign *equatorial* and *axial* descriptors to the solution-state major and minor *N*-methyl diastereomeric species of *N*-methylpiperidine-type molecules incapable of ring-inversion, such as **8**, **15** (X^- = $HOSO_3^-$ and $CH_3SO_3^-$, racemic), **14** and **16**, X^- = $CH_3SO_3^-$. For example, *equatorial* descriptors were assigned to *N*-methyl carbons of the **16** (X^- = $CH_3SO_3^-$) major species [δ 42.33 (D_2O) and 42.24 (CD_2Cl_2)] and *axial* descriptors to the *N*-methyl carbons of the minor species [δ 33.49 (D_2O) and 33.07 (CD_2Cl_2)] in the appropriate solvent.[25]

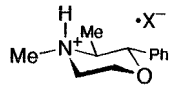

In a similar manner, one can assign *equatorial*/*axial* [and also ring-invertomeric (*M*,*P*)] descriptors to the

(19) Blunt, J. *Boltzmann Distribution HyperCard Stack*, University of Canterbury: Christchurch, New Zealand, 1989.

(20) Glaser, R.; Hug, P.; Drouin, M.; Michel, A. *J. Chem. Soc., Perkin Trans. 2* **1992**, 1071.
(21) Michel, A.; Drouin, M.; Glaser, R. *J. Pharm. Sci.* **1994**, *83*, 508.
(22) Kussäther, von E.; Hasse, J. *Acta Crystallogr.* **1972**, *B28*, 2896.

solution-sate major and minor *N*-methyl diastereomeric species of *N*-methylpiperidine-type molecules which show a strong conformational bias against ring-inversion. This can be done even if the conformational bias is not exactly 100% in favor of only one particular invertomer, provided that there is a *significant* predominance of one piperidine ring invertomer to the time-averaged structure of a solution-state *N*-methyl diastereomeric species. It will be shown that while, under the conditions of our NMR measurements, epimers **2**, **3** in D_2O and CD_2Cl_2 solutions do indeed exhibit varying degrees of bias against ring-inversion, this bias is always strongly in favor of one of the two ring-invertomeric possibilities [as shown by piperidinyl ring ^3J(HH) coupling constants].

A general method will be used for the assignment of *axial*/*equatorial* stereochemical descriptors for the *N*-methyl and CH(Ph)COOMe groups. In this method, *axial*/*equatorial N*-methyl descriptors will be made based upon the relative ^{13}C chemical shifts of the *N*-methyl nuclei and their agreement with values from molecules of known stereochemistry based upon X-ray crystallography/solid-state cpmas spectroscopy [see above]. In CD_2Cl_2 solutions these assignments will be confirmed, where possible, by comparing the vicinal coupling constants involving the *N*-H proton. Thus, an *axial N*-methyl group would have an *equatorial N*-H proton which has *synclinal* relationships to each one of the C(5) methylene protons [H(4)···H(51) and H(4)···H(52)]. As a result, one would expect two small [*ca.* 2.5 Hz] and approximately equal ^3J(4−51) and ^3J(4−52) coupling constants. An *equatorial N*-methyl group, on the other hand, would have an *axial N*-H proton which has one *antiperiplanar* and one *synclinal* relationship to the C(5) protons. For example, these relationships would afford one large [*ca.* 9−10 Hz, ^3J(4−51)] and one small [*ca.* 2.5 Hz, ^3J(4−52)] coupling constant in an (*M*)-invertomer.

The assignment of *axial*/*equatorial* stereochemical descriptors for the CH(Ph)COOMe moieties ligated to C(3) will be based, where possible, upon the coupling constants involving H(3) and its vicinal neighbors. Therefore, an *equatorial* CH(Ph)COOMe substituent would have an *axial* H(3) which has one *antiperiplanar* and one *synclinal* relationship to the C(8) methylene protons. An *axial* CH(Ph)COOMe substituent would have an *equatorial* H(3) which has a *synclinal* relationship to each one of the C(8) methylene protons. In CD_2Cl_2 solutions, confirmation of the substituent assignments can also be made, where possible, by measurement of ^3J(3−4). A *diequatorial* relationship between the 3,4-ring substituents would have H(3) and H(4) *diaxial* and thus give rise to a large *antiperiplanar*-magnitude ^3J(3−4) value, while 3-*equatorial*-4-*axial* substitution would result in a small *synclinal*-type ^3J(3−4) value.

A conformational bias against ring-inversion can be measured by the relative size of the vicinal coupling constants in dimethylene fragments of the piperidine ring. For example, there is one *antiperiplanar* [H(51)···H(61)], and three *synclinal* relationships [H(51)···H(62), H(52)···H(61), H(52)···H(62)] in the (*M*)-invertomer, *i.e.* one large and three small vicinal coupling constants. Ring-inversion interconverts the *axial*/*equatorial* orientation of protons. Thus, the H(51)···H(61) relationship would be now be *synclinal* in the (*P*)-invertomer, H(52)···H(62) would be *antiperiplanar*, while H(51)···H(62) and H(52)···H(61) would remain *synclinal*. Measurement of two similar "averaged" magnitudes for ^3J(51−61) and ^3J(52−62) would testify to rapid ring-inversion between (*M*) and (*P*), while a large value for ^3J(51−61) and a small one for ^3J(52−62) would signify a bias for the (*M*)-invertomer according to the numbering scheme in Figure 2.

Piperidine-Ring Conformation of Major D_2O [and Minor CD_2Cl_2] Species (2*RS*,3*RS*,4*RS*,*MP*)-2. The δ 32.82 and 41.00 *N*-methyl carbon signals in a 5:4 ratio for **2** in D_2O strongly suggest *axial* and *equatorial N*-methyl dispositions in the respective major and minor species. The large 11.4(1) Hz *antiperiplanar*-type ^3J(3−81) and smaller 2.5(1) Hz *synclinal*-type ^3J(3−82) values measured for the major D_2O species are inconsistent with time-averaging due to rapid ring-inversion, and their magnitudes point to *antiperiplanar* H(3)···H(81) and *synclinal* H(3)···H(82) relationships. As a result, H(3) and H(81) are *diaxial* and the CH(Ph)$COOCH_3$ moiety on C(3) can now be assigned an *equatorial* descriptor. The same above-mentioned *axial N*-methyl/*equatorial*-CH(Ph)$COOCH_3$ (2*RS*,3*RS*,4*RS*,*MP*)-**2** diastereomer is present in CD_2Cl_2 solution, but now it is the minor species [as shown by the similar list of ^{13}C chemical shift values reported in Table 2]. Comparison of the 11.4(1) Hz *antiperiplanar*-magnitude value noted for the major species of **2** with the corresponding 11.6(1)[25] Hz value for the major species C$\underline{H}_2$C$\underline{H}_2$ fragment of **16** ($X^- = CH_3SO_3^-$) in CD_2Cl_2 clearly shows that both molecules are conformationally biased against ring-inversion.

It will be shown below that also for **3**, the *axial N*-methyl/*equatorial*-CH(Ph)$COOCH_3$ diastereomer is the major species in D_2O, while it is the minor one in CD_2Cl_2 solution. Similarly, for both **2** and **3**, the *equatorial N*-methyl/*equatorial*-CH(Ph)$COOCH_3$ epimer is the minor species in D_2O and becomes the major one in CD_2Cl_2 medium. A analogous solvent dependency was noted for the relative amounts of *equatorial* and *axial N*-methyl diastereomers of **8** in D_2O and CD_2Cl_2.[15]

Piperidine-Ring Conformation of Minor D_2O [and Major CD_2Cl_2] Species (2*RS*,3*RS*,4*SR*,*MP*)-2. The δ 41.00 and 41.63 values for the *N*-methyl carbon in the respective minor D_2O and major CD_2Cl_2 species clearly point to similar *equatorial* dispositions of this substituent. Placement of N^+ in the coupling path reduces the magnitudes of vicinal coupling constants involving *N*-H.[26] For example, in **16**, $X^- = CH_3SO_3^-$, typical 4.9(1) and 6.5(1) Hz values were measured for the respective ^3J(N-$\underline{H}$C$\underline{H}_3$) and ^3J(C$\underline{H}$C$\underline{H}_3$) coupling constants.[25] The **2** major species *axial N*-H proton is mutually *antiperiplanar* to both its H(3) and H(51) neighbors [as shown by the 8.3(2) Hz ^3J(3−4) and 9.4(2) Hz ^3J(4−51) coupling constants], while it is *synclinal* to H(52) [as shown by the smaller 1.6(1) Hz value for ^3J(4−52)]. These three values compare nicely with the corresponding ones [9.0(1), 9.8(1), and 2.5(1) Hz] measured for the respective ^3J(NHCH) coupling constants in *equatorial N*-methyl **16** ($X^- = CH_3SO_3^-$) which is conformationally biased against ring-inversion due to *diequatorial* phenyl/methyl substituents on the piperidine ring.[25] Since H(3) is *antiperiplanar* to

(23) Glaser, R.; Adin, I.; Drouin, M.; Michel, A. *Struct. Chem.* **1994**, *5*, 197.
(24) Glaser, R.; Shiftan, D. Unpublished results; water content of hydrated molecule was not determined in ref 15.
(25) Glaser, R. *Magn. Reson. Chem.* **1989**, *27*, 1142.
(26) Fraser, R. R.; Renaud, R. N.; Saunders, J. K.; Wigfield, Y. Y. *Can. J. Chem.* **1973**, *51*, 2433.

H(4) and also to H(81) [12.1(2) Hz $^3J(3-81)$], it follows that the CH(Ph)COOMe moiety is also *equatorially* oriented in the major CD_2Cl_2 species of **2**. One may then affix the (2*RS*,3*RS*,4*SR*,*MP*)-**2** descriptor to the major species in CD_2Cl_2 and also to the minor species in D_2O. The observation of coupling involving *N*-H and its vicinal neighbors [*e.g.* those noted above and the 4.9(1), 4.8(1) Hz $^3J(4-9)$ values for both major and minor CD_2Cl_2 species of **2**] readily testifies that ^+N-H bond breaking and bond making processes are at the SEL in this solvent.

The large 12.7(2), 11.5(3), 12.9(3), and 12.1(3) Hz *antiperiplanar*-type values for the CD_2Cl_2 major species respective $^3J(51-61)$, $^3J(61-71)$, $^3J(71-81)$, and $^3J(3-81)$ coupling constants strongly point to a *chair* conformation piperidinyl ring in which not only are H(3), H(51), H(61), H(71), and H(81) all *axial* [in addition to H(4)], but the large magnitudes of these values themselves argue against significant averaging resulting from ring-inversion. Measurements of long-range 2.4(1) Hz $^4J(52-72)$ and 3.0(4) $^4J(62-82)$ "W"-type coupling constants are consistent with a rigid piperidine ring in CD_2Cl_2. The original Karplus relationship[27] for vicinal coupling constants does not take into consideration the orientation and electronegativity of X,Y substituents in CH(X)−CH(Y) segments.[28] Altona and co-workers[28] have produced a generalized Karplus relationship which takes these effects into consideration, while Lambert[29] has shown that these effects are effectively canceled by using a ratio (*R*) of *trans:cis* coupling constants [$R = (^3J_{axax} + {}^3J_{eqeq})/(^3J_{axeq} + {}^3J_{eqax})$]. Using Lambert's ratio method and the appropriate coupling constants,[29] the solution-state N−C(5)−C(6)−C(7) and C(6)−C(7)−C(8)−C(3) dihedral angles can be estimated to be 58(1)° and 60(2)°, respectively [compared to 56° and 57°, respectively, in the MM3 model of *antiperiplanar* H(2)···H(3) (model **9**) for (2*R*,3*R*,4*S*,*M*)-**2**].

However, there are some subtle differences between the (2*RS*,3*RS*,4*SR*,*MP*)-**2** major species in CD_2Cl_2 and the corresponding minor species in D_2O. While there is clearly a conformational bias against ring-inversion for the (2*RS*,3*RS*,4*SR*,*MP*)-**2** major species in CD_2Cl_2, this does not appear to be the case for the minor species in D_2O. The smaller 9.6(1) and 8.3(3) Hz magnitudes for the D_2O minor species respective $^3J(51-61)$ and $^3J(3-81)$ coupling constants can arise from time-averaging due to ring-inversion. As such, these coupling constant magnitudes suggest that while the *diequatorial* (2*RS*,3*RS*,4*SR*,*MP*)-**2** ring-invertomer predominates in both CD_2Cl_2 and D_2O, its extent is slightly diminished in the latter solvent via a small contribution from the *diaxial* (*PM*) diastereomer.

Piperidine-Ring Conformation of Major (2*SR*,3*RS*,4*RS*,*MP*)-3 and Minor (2*SR*,3*RS*,4*SR*,*MP*)-3 Species in D_2O. Using argumentation similar to that presented above, one can characterize the D_2O major and minor species of **3** as having δ 32.02 *axial* and δ 40.87 *equatorial* *N*-methyl carbons, respectively. Since the major species exhibits *antiperiplanar*-magnitude 11.3(1) $^3J(2-3)$ and 13.2(2) Hz $^3J(51-61)$ values, and the corresponding values for the minor species are 9.0(5) and 10.3(4) Hz, one may affix *equatorial* descriptors to the CH(Ph)COOMe moieties of both the *chair* conformation major and minor *N*-methyl diastereomers, as in the case of the corresponding *threo* epimer **2**. Also analogous to **2**, while the magnitudes of these coupling constants show a preponderance of one ring-invertomer [(2*SR*,3*RS*,4*RS*,*MP*)-**3** for the major species and (2*SR*,3*RS*,4*SR*,*MP*)-**3** for the minor species] to the respective time-averaged structures, there appears to be slightly more of a small contribution from the relevant (*PM*) ring-invertomer to the minor D_2O species than to the major one.

Piperidine-Ring Conformation of Major (2*SR*,3*RS*,4*SR*,*MP*)-3 and Minor (2*SR*,3*RS*,4*RS*,*MP*)-3 Species in CD_2Cl_2. Once again the δ 44.28 major and δ 36.12 minor species ^{13}C chemical shifts point to *equatorial* and *axial* *N*-methyl orientations, respectively. The major species *axial* *N*-H proton is mutually *antiperiplanar* to both its H(3) and H(51) neighbors [as shown by the 8.7(4) Hz $^3J(3-4)$ and 9.2(2) Hz $^3J(4-51)$ coupling constants]. Since the major species H(3) is *antiperiplanar* also to H(81) [11.5(3) Hz $^3J(3-81)$], it follows that the CH(Ph)COOMe moiety is also *equatorially* oriented in the major CD_2Cl_2 species of **3**. One may thus affix *diequatorial* (2*SR*,3*RS*,4*SR*,*MP*)-**3** descriptors to the major species in CD_2Cl_2. The δ 51.47 C(2) and 65.35 C(3) chemical shifts for the *axial* *N*-methyl minor CD_2Cl_2 species compared to the corresponding δ 52.57 C(2) and 63.22 C(3) values measured for the *axial* *N*-methyl/*equatorial*-CH(Ph)COOMe major D_2O species of **3** suggests that both share the same (2*SR*,3*RS*,4*RS*,*MP*)-**3** piperidine-ring conformation and configuration.

Similar to the case of the *diequatorial* major **2** species in CD_2Cl_2 noted above, the large 12.6(2) $^3J(51-61)$ and 13.7(6) $^3J(61-71)$ values for the corresponding *diequatorial* major *erythro*-**3** species in CD_2Cl_2 point to a marked bias of the (*MP*) invertomer against ring-inversion in this organic solvent. *Therefore, we have shown above that the (MP)-piperidine ring major **2** and **3** species in either D_2O or CD_2Cl_2 are biased against ring-inversion, while the minor species in these same solvents exhibit a small amount of (PM) contribution to the predominant (MP)-invertomer.*

C(2)−C(3) Bond Conformation. The $^3J(2-3)$ coupling constant is obviously diagnostic for the conformational preferences in the C(2)−C(3) bond rotamer mixtures for **2** and for **3** in each solvent. These coupling constants are all in accord with those from predominant rotamers whose spatial arrangements avoid g^+/g^- interactions, as noted above. The measurement of 11.0(1) and 11.6(1) Hz values for the *axial* *N*-methyl/*equatorial*-CH(Ph)COOMe major D_2O species of **2** and **3**, respectively, clearly points to a predominant contribution from the *antiperiplanar* H(2)···H(3) rotamer in both cases [*e.g.* model **9** for (2*R*,3*R*,4*R*,*M*)-**2** and model **10** for (2*S*,3*R*,4*R*,*M*)-**3**]. The estimated Boltzmann distributions (see Table 3) of 98% calculated for model **9** and 95% for model **10** are undoubtedly consistent with the experimental results. Using estimated vicinal coupling constants based upon Altona's[28,30] generalized Karplus relationship, and the estimated Boltzmann distributions, weighted time-averaged values of 11.8 and 11.5 Hz were calculated for the

(27) Karplus, M. *J. Chem. Phys.* **1959**, *30*, 11. *J. Am. Chem. Soc.* **1963**, *85*, 2870.

(28) Haasnoot, C. A. G.; de Leeuw, F. A. A. M.; Altona, C. *Tetrahedron* **1980**, *36*, 2783.

(29) Lambert, J. B. *J. Am. Chem. Soc.* **1967**, *89*, 1836. *Acc. Chem. Res.* **1971**, *4*, 87.

(30) Blunt, J. *HyperCard Stack for Altona's Generalized Karplus Relationship*, University of Canterbury: Christchurch, New Zealand, 1988.

major D_2O species of **2** and **3**, respectively. A second estimation of the Boltzmann distribution of the three staggered rotamers was made based upon semiempirical AM1/COSMO[31] energy optimized molecular modeling calculations (DE = 78.5). Molecular orbital calculations using COSMO involve dielectric screening in solvents with explicit expressions for the screening energy and its gradient.[32] The AM1/COSMO estimated *antiperiplanar* H(2)···H(3) rotamer Boltzmann distribution of 98% [model **9**-type] is in excellent agreement with that calculated by MM3 (DE = 80), and its value is consistent with that expected from the averaged 11.0 Hz $^3J(2-3)$ coupling constant. However, the corresponding 79% value estimated by AM1/COSMO for the *erythro* model **10**-type is lower than the 95% calculated by MM3 and is also lower than that expected from the observed 11.6(1) Hz $^3J(2-3)$ averaged coupling constant.

The 7.7(1) and 5.9(3) Hz $^3J(2-3)$ averaged coupling constant measured for the *diequatorial N*-methyl/-CH(Ph)COOMe major D_2O species of **2** and **3**, respectively, clearly point to a large reduction in the amount of the *antiperiplanar* H(2)···H(3) rotamer. The Boltzmann distributions estimated from MM3 calculated *diequatorial* models [*ca.* 48% (+)-*synclinal* H(2)···H(3) (model **11**) and 42% *antiperiplanar* H(2)···H(3) (model **13**) for the *equatorial N*-methyl (2*R*,3*R*,4*S*,*M*)-**2** set; *ca.* 84% (+)-*synclinal* (model **12**) H(2)···H(3) for the *equatorial N*-methyl (2*S*,3*R*,4*S*,*M*)-**3** set] are also in accord with the experimental findings. Therefore, *relative* contributions of C(2)−C(3) bond rotamers based upon their estimated populations within a conformational set are *all* in agreement with those expected from the time-averaged coupling constants, despite possible underestimation in MM3 (DE = 80) stability for species capable of internal hydrogen-bonding.

Bioactive Conformation of 2. The receptor environment of a molecule may influence the relative energies of different conformers. However, it is unlikely that a conformer that is more than 1 or 2 kcal/mol above the global minimum would be the bioactive form since a high energy form binding to the receptor would be expected to cause a large decrease in the binding affinity of the compound. Inspection of Table 3 shows that numerous conformations reside within this energy gap. The pharmacophoric hypothesis for inhibition of dopamine reuptake by the secondary amine **1** involves a coplanar relationship between N−H and C(1)−C(2) bonds. This auspicious geometry exists in both the *equatorial* CH(Ph)COOMe (2*R*,3*R*,*M*)-**1** and the *axial* CH(Ph)COOMe (2*R*,3*R*,*P*)-**1** ring-invertomers. The *equatorial* N−H(*pro-S*) and *equatorial* C(1)−C(2) bonds are coplanar in the conformationally favored piperidine ring (2*R*,3*R*,*M*)-**1** diastereomer in Figure 1, while the *equatorial* N−H(*pro-R*) and *axial* C(1)−C(2) bonds now have this relationship in the (2*R*,3*R*,*P*)-**1** invertomer. Inspection of the four tertiary amine *threo*-diastereomers **2** in Figure 2 shows that this favorable relationship exists only in *axial N*-methyl/*equatorial* CH(Ph)COOMe (2*R*,3*R*,4*R*,*M*)-**2** and in *axial N*-methyl/*axial* CH(Ph)COOMe (2*R*,3*R*,4*S*,*P*)-**2**, while the N−H bond is predicted to be inappropriately orientated in *equatorial N*-methyl/*equatorial* CH(Ph)COOMe (2*R*,3*R*,4*S*,*M*)-**2** and in *equatorial N*-methyl/*axial* CH(Ph)COOMe (2*R*,3*R*,4*R*,*P*)-**2**. Since the unfavorable N−H oriented *equatorial N*-methyl/*equatorial* CH(Ph)COOMe (2*R*,3*R*,4*S*,*M*)-**2** diastereomer has a considerable population in both D_2O (*ca.* 45%) and in CD_2Cl_2 (*ca.* 87%) solutions, one can now rationalize the experimentally observed lowered pharmacologic activity found upon *N*-methylation of **1**.

Experimental Section

(±)-*threo*-*N*-Methyl-α-phenyl-2-piperidineacetic acid methyl ester (**2**), (±)-*erythro*-*N*-methyl-α-phenyl-2-piperidineacetic acid methyl ester (**3**), and (±)-*threo*-*N*,*p*-dimethyl-α-phenyl-2-piperidineacetic acid methyl ester (**5**) were synthesized, as previously described,[8] by reductive amination of the corresponding secondary amines.

Crystallography. Crystallographic measurements were made on a Siemens P4 automatic diffractometer with graphite-monochromated Cu Kα radiation. Data crystals were mounted on glass fibers and fixed on a goniometer head on the X-ray diffractometer. Data were collected at 233 K (for **2**) and 293 K (for **5**) using the 2 θ/ω scan technique to a maximum 2θ value of 114.5°. Scans were made with a variable speed of 7.5−30 deg min^{-1} and a background time/scan time ratio of 0.5. Space group determination was based upon systematic absences, packing considerations, a statistical analysis of intensity distribution, and the succcessful solution and refinement of the structure. XSCANS[33] software was used for centering, indexing and data collection, and SHEXTLPC[34] software was used for crystal structure solution by application of direct methods and refinement by least squares on F^2. Atomic scattering factors stored in the SHEXTLPC[34] program were those of Cromer and Waber.[35]

X-ray Crystallography of 2. Crystallization was performed by vapor diffusion of petroleum ether into an ethyl acetate solution of **2**. A clear, colorless plate crystal of $C_{15}H_{22}ClNO_2$ having approximate dimensions 0.24 × 0.32 × 0.42 mm was chosen. Cell constants and an orientation matrix for data collection, obtained from a least-squares refinement using the setting angles of 35 carefully centered reflections in the range 11° ≤ 2θ ≤ 55°, corresponded to a monoclinic system $P2_1$ cell with dimensions at 233 K of a = 8.843(1), b = 18.406(4), c = 9.158(2) Å, β = 90.33(2)°, V = 1490.6(5) Å^3. For Z = 4 and FW = 283.79, the calculated density is 1.265 g cm^{-3}. The determination of a chiral space group ($P2_1$) showed that spontaneous resolution had occurred to afford chiral crystals.

Decay of 1.2% was measured and corrected accordingly. An isotropic extinction coefficient was included in the refinement to account for secondary extinction effects;[36] its value was 0.0061(10). Since the minimum and maximum transmission factors were 0.36 and 0.65, a face indexed integration absorption correction was applied. Structure determination afforded two independent disordered structures (**6** and **6′**). The occupancy factors for atoms C(5A/B), C(6A/B), C(7A/B), C(8A/B), and C(9A/B) in each of these two independent structures were refined. Upon convergence, the relative occupation of molecules A:B was found to be 0.710(7):0.290(7). Hydrogens were all placed at calculated positions and refined using the riding model method, while non-hydrogen atoms were refined anisotropically [with the exception of atoms C(5B), C(6B), C(7B), C(8B), and C(9B) in the **2-B** and **2′-B** molecules which were refined isotropically]. At convergence the final discrepancy indices on F were $R(F)$ = 0.036, $_wR(F^2)$ = 0.125, and GOF

(31) *CS-Chem3D Pro 3.5.1/CS-Mopac Pro for ChemOffice 4.0*, CambridgeSoft: Cambridge, MA, 1997.

(32) Klamt, A.; Schüurmann, G. *J. Chem. Soc. Perkin Trans. 2* **1993**, 799.

(33) *XSCANS 2.2*, Siemens Analytical X-ray Instruments Inc.: Madison, WI, 1996.

(34) *SHEXTLPC 5.0*, Siemens Analytical X-ray Instruments Inc.: Madison, WI, 1995.

(35) Cromer, D. T., Waber, J. T. In *International Tables for X-ray Crystallography*; Ibers, J. A., Hamilton, W. C., Eds., Kynoch Press: Birmingham, 1974; Vol. IV, pp 99−101, Table 2.2B. (Present distributor Kluwer Academic Publishers: Dordrecht.)

(36) Larson, A. C. *Crystallographic Computing*, Munksgaard: Copenhagen, 1970; p 291.

= 1.07 for the 2126 reflections with $I_{net} \geq 2\sigma(I_{net})$ and 398 parameters refined with 25 restraints.

X-ray Crystallography of 5. Crystallization was performed by slow evaporation from a butan-2-one/octane solution of **5**. A clear, colorless plate crystal of $C_{16}H_{24}ClNO_2$ having approximate dimensions 0.06 × 0.28 × 0.52 mm was chosen. Cell constants and an orientation matrix for data collection, obtained from a least-squares refinement using the setting angles of 35 carefully centered reflections in the range $9.2° \leq 2\theta \leq 54.6°$, corresponded to a monoclinic system *C*2/*c* cell with dimensions at 293 K: $a = 19.274(2)$, $b = 10.087(2)$, $c = 16.363(2)$ Å, $\beta = 100.124(9)°$, $V = 3131.6(7)$ Å. For $Z = 8$ and FW = 297.81, the calculated density is 1.263 g cm^{-3}.

Decay of 1.7% was measured and corrected accordingly. Since the minimum and maximum transmission factors were 0.46 and 0.88, a face indexed integration absorption correction was applied. Hydrogens were all placed at calculated positions and refined using the riding model method, while non-hydrogen atoms were refined anisotropically. At convergence the final discrepancy indices on *F* were $R(F) = 0.062$, $_wR(F^2) = 0.162$, and GOF = 1.06 for the 1670 reflections with $I_{net} \geq 2\sigma(I_{net})$ and 184 variables.

NMR Spectroscopy. ^{1}H (500.13 MHz) and ^{13}C (125.76 MHz) NMR spectra were measured at 11.7 T on a Bruker DMX-500 Fourier transform spectrometer in either D_2O or CD_2Cl_2 solvent at 298 K. The deuterated solvent was used as an internal lock, residual protio $CDHCl_2$ solvent was used as an internal secondary reference for spectra of the salts recorded in CD_2Cl_2 [δ_H 5.32 and δ_C 53.8 relative to tetramethylsilane], and 4,4-dimethyl-4-silapentanesulfonate sodium salt was used as the spectral reference in D_2O. Standard Bruker DEPT (90° and 135° pulse angles) pulse programs were used to establish the hydrogen multiplicity of the ^{13}C signals and HMQC 2D ^{1}H/^{13}C correlation.

Molecular Modeling. The energy-minimized geometries of various species were determined by the MM3(92) program[18,37] provided with the MACMIMIC 3.0 package.[13] Only chair conformations of the piperidine ring were considered since these are generally strongly preferred. Also, since only chair conformers were experimentally observed, it was felt to be unnecessary to explore other possible conformations of the piperidine ring. A high dielectric constant (DE = 80) in the MM3(92) calculations was chosen to provide a qualitative assessment of the effects of a polar solvent. Semiempirical molecular orbital AM1/COSMO [keyword: EPS = 78.5] energy optimized molecular models were obtained using the CS-CHEM3D PRO 3.5.1/CS-MOPAC PRO program combination.[31] Calculations were performed on a Macintosh Quadra 950 workstation equipped with an Apple PowerMacintosh upgrade card. Iconic projections of the X-ray crystallographic or molecular modeling structures were generated using the combination of CS-CHEM3D PRO 3.5.1[31] and CS-CHEMDRAW PRO 4.0.1[38] programs.

Acknowledgment. The Bruker DMX-500 spectrometer at The University Laboratory for Magnetic Resonance (Ben-Gurion University of the Negev) was purchased with a matching funds grant from the Israel Ministry of Science and Industry. R.G. would like to acknowledge that part of these investigations were performed at the Institute for Advanced Studies at the Hebrew University of Jerusalem as an Institute Fellow in the study group on Chirality and Chiral Drugs. This work was presented by I.A. and D.S. in partial fulfillment of the Ph.D. requirements at Ben-Gurion University of the Negev. Part of this work was supported by National Institute of Drug Abuse contract N01DA-4-8313 to M.F., grant DA06305 to H.M.D., and contract DA09045 to C.G. C.G. would also like to acknowledge the support of the Naval Research Laboratory.

Supporting Information Available: The crystallographic details, fractional coordinates for non-hydrogen and hydrogen atoms, interatomic bond distances, bond angles, torsion angles, and anisotropic thermal parameters for **2** and **5** (17 pages). This material is contained in libraries on microfiche, immediately follows this article in the microfilm version of the journal, and can be ordered from the ACS; see any current masthead page for ordering information.

JO971063B

(37) Allinger, N. L.; Yuh, Y. H.; Lii, J.-H. *J. Am. Chem. Soc.* **1989**, *111*, 8551.

(38) *CS ChemDraw Pro 4.0.1 for ChemOffice 4.0*, CambridgeSoft: Cambridge, MA, 1997.